SCALING AND CORRELATION OF FLUCTUATING VORTICITY IN TURBULENT WALL LAYERS

Ronald L. Panton
Department of Mechanical Engineering
University of Texas
Austin, TX 78712
rpanton@mail.utexas.edu

ABSTRACT

Asymptotic expansions for the profiles of fluctuating vorticity in boundary layers are proposed based on DNS data. The inner region requires two terms with different scalings; $<\omega_i\omega_i>/(U_0 u_\tau^3/\nu^2)$ and $<\omega_i\omega_i>/(u_\tau^4/\nu^2)$. The first term decays exponentially and needs no matching term in the outer region. The second term has an overlap behavior of ~ C/y^+ . To match the outer region this requires a third scaling for the outer expansion $<\omega_i\omega_i>/(u_\tau^3/\nu\delta)$. This scaling turns out to be the Kolmogorov time scale.

INTRODUCTION

From a mathematical viewpoint the theory of turbulent wall layers is a singular perturbation problem for large Reynolds numbers. Profiles are expressed as matched asymptotic expansions. There are three parts; an expansion for the outer region, an expansion for the inner region, and a common part that matches the two.

The velocity profile is a well-known example. For the outer region the profile has an expansion consisting of two terms.

$$\frac{U}{U_0}(Y,\mathrm{Re}_\tau) \sim 1+F(Y)\frac{u_\tau}{U_0}(\mathrm{Re}_\tau)+\ldots \qquad as\ \mathrm{Re}_\tau \to \infty \tag{1}$$

The gauge function u_τ/U_0 approaches zero as Re_τ becomes large according to

$$\frac{u_\tau}{U_0}=1/\left[\frac{1}{\kappa}\ln(\mathrm{Re}_\tau)+C_i-C_0\right] \tag{2}$$

It also changes the scaling of the F(Y) term in (1) compared to the leading term.

The inner region profile has only the second term in the series.

$$\frac{U}{U_0}(y^+,\mathrm{Re}_\tau) \sim f(y^+)\frac{u_\tau}{U_0}(\mathrm{Re}_\tau)+\ldots \tag{3}$$

The limiting behavior, the common part, is the log law.

$$F_{CP}=\frac{U-U_0}{u_\tau}\sim\frac{1}{\kappa}\ln(Y)+C_o \qquad Y\to 0$$
$$\left.\frac{U}{u_\tau}\right|_{CP}\sim\frac{1}{\kappa}\ln(y^+)+C_i \qquad y^+\to\infty \tag{4}$$

These common parts were found by Izakson(1937) and Millikan(1938) by requiring that equations (1) and (3) match in an overlap region. This was a significant change in viewpoint as it renders moot the quasi-physical assumptions and arguments previously used to derive log laws.

A uniformly valid profile is represented as a composite expansion. An additive composite expansion is the sum of the inner and outer expansions minus the common part. For example, consider the Reynolds shear stress has the composite expansion;

$$-<uv>^+\equiv-\frac{<uv>}{u_\tau^2}=g(y^+)+G(Y)-1 \tag{5}$$

Here the inner Reynolds shear stress function is g(y+) and the outer is G(Y). The common part is found to be

$$g_{cp}=g(y^+\to\infty)=G_{cp}=G(Y\to 0)=1 \tag{6}$$

Equation 5 contains a Reynolds number effect because $Y=y^+/Re_\tau$.

Figures 1 displays the Reynolds stress $-<uv>^+$ from the DNS of Schlatter et al. (2010) in outer variables. The Reynolds number effects in Fig. 1 are evident. The solid black line is an estiment for *G(Y)*. The inner stress function $g(y^+)$ is plotted in Fig. 2. This was produced by solving Eq. 5 for $g(y^+)$, substituting data for $<uv>^+$, and the estimate for *G(Y)* from Fig.1. A reasonably good correlation is obtained. The DNS data and the prediction of Eq 5 for $-<uv>^+$ are displayed on Fig. 3. The prediction matches well except in the outer region at the lowest Reynolds , $Re_\tau=250$.

Fig.1 Reynolds Shear Stress; Outer Function

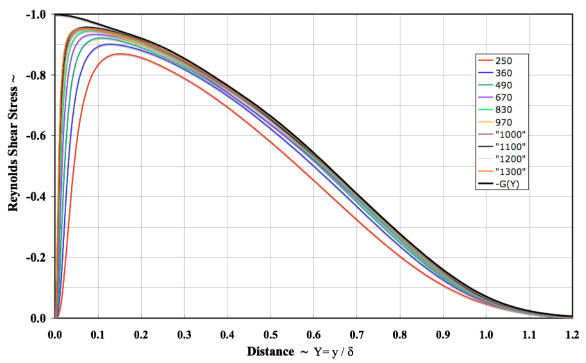

Fig.2 Reynolds Shear Stress; Inner Function

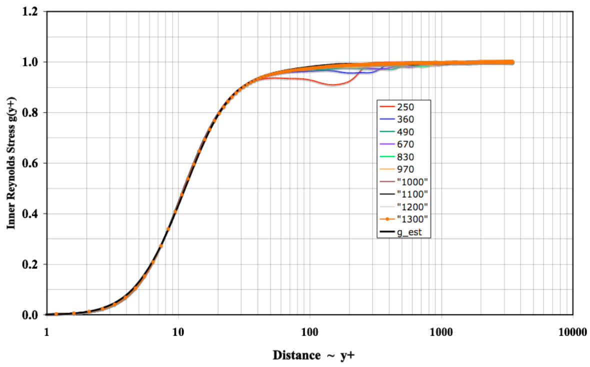

Fig.3 Reynolds Shear Stress; DNS & Composite

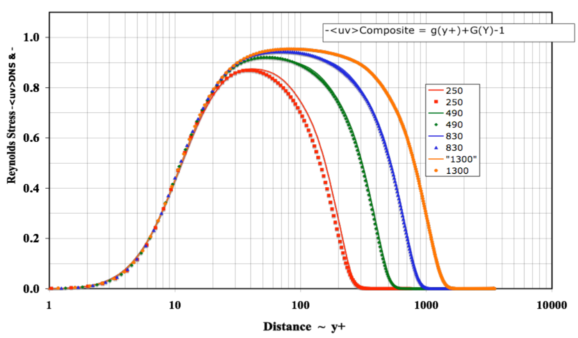

Vortical and Irrotational Fluctuations

It has been observed that a turbulent boundary layer has regions of vortical fluid and regions where the flow is an irrotational potential flow. Experimental measurements show fluctuations are intermittent between irrotational and vortical out to y/δ ~ 1.2. DNS results yield an rms vorticity fluctuation decrease by a factor of 100 at about y/δ ~ 1.5 . Potential fluctuations extend somewhat further out. The streamwise velocity rms decreases by a factor of 100 at about y/δ ~ 2.0

By the Helmholtz decomposition and Biot-Savart law one can propose that everywhere the velocity fluctuations can be decomposed into potential and vortical parts.

$$\mathbf{u} = \mathbf{u}^{(\phi)} - \frac{1}{4\pi}\int \frac{\mathbf{r}\times\omega'}{|r|^3}\, dV' \tag{7}$$

The potential component is caused by singularities within the boundary. Also note that the integral produces potential motions in regions away from where the vorticity exists. The intimate connection between velocity and vorticity is explicit in Eq. 7.

Corrsin and Kistler(1954) derived (see Pope (2000)) a significant relation regarding fluctuating irrotational motions. Let the kinetic energy be $k \equiv \frac{1}{2} < u_i^{(\phi)} u_i^{(\phi)} >$. Then, the net Reynolds stress for irrotational fluctuations is equal to the gradient of the kinetic energy.

$$\frac{\partial}{\partial x_i} < u_i^{(\phi)} u_j^{(\phi)} > = \frac{\partial k}{\partial x_j} = \frac{\partial(\delta_{ij} k)}{\partial x_i}$$
$$< u_i^{(\phi)} u_j^{(\phi)} > = \delta_{ij} k \tag{8}$$

The Reynolds stress of irrotational fluctuations is equivalent to a pressure and has no effect on the mean velocity profile.

Townsend(1972) in his second book defined active motions as those that make an essential contribution to the Reynolds shear stress. Thus, potential motions are inactive. However, there may also be vortical motions that are inactive as defined by Townsend. Active and inactive are useful catagories, but are not rigorously defined.

Different Velocity Scales

The Reynolds shear stress $<uv>$ scales when normalized with the friction velocity. However, there is much evidence (for instance Degraaff and Eaton (2000)) that some fluctuations, such as the streamwise velocity $<uu>$, scale with the mixed velocity $\sqrt{u_\tau U_0}$. Perhaps the first use of this scale was Alfredsson and Johansson(1984).

It has also been found that the fluctuating wall shear stress, which is directly related to the fluctuating wall vorticity does not scale on the friction velocity.

Because u_τ and U_0 separate as the Reynolds number increases, quantities that scale differently will also sepearate. The ratio $u_\tau/U_0(Re_\tau)$ as a gauge function changes the scaling of the terms. An asymptotic expansion of the quantity will have two terms to account for the different scaling behavior.

The free stream velocity does not usually appear in inner region quantities, however, the outer region potential motions can be imposed at the wall through pressure fluctuations.

Data Sources

The first DNS boundary layer analysis was Spalart (1988). Data for the present analysis comes from DNS calculations of Jiménez et al. (2010) and Schlatter et. al. (2011). Channel flow DNS data comes from Kim et al. (1987), from Jiménez and coworkers (2003, 2004, 2006, 2008)), and Morishita et al. (2011). DNS data has good internal consistency,. However, Schlatter and Orlu (2010), especially for boundary layers, note differences between different calculations and urge caution.

INNER REGION

Consider that the $<uv>$ and $<vv>$ correlations scale with u_τ, however, the $<uu>$ correlation scales approximately with $\sqrt{u_\tau U_0}$. The streamwise velocity u has two types of activity; active and inactive. An asymptotic expansion for $<uu>$ needs two terms in order to account for the different scaling.

The central point of this paper is that an adequate representation of vorticity fluctuations in the inner region also requires an asymptotic expansion of two terms. This form is (using i as a general index without implying a sum):

$$\frac{<\omega_i\omega_i>}{U_0 u_\tau^3/\nu^2} \sim \frac{<\omega_i\omega_i>_0}{U_0 u_\tau^3/\nu^2}(y^+) + \frac{<\omega_i\omega_i>_1}{u_\tau^4/\nu^2}(y^+)\bullet\frac{u_\tau}{U_0}(\mathrm{Re}_\tau)$$

(9)

The Reynolds number relation for the gauge function was alteady given in Eq. 2. It is convenient to define some symbols for the nondimensional forms. Number subscripts, 0 and 1, indicate the term order in the expansion, while the superscript + is friction velocity scaling and # is mixed scaling.

$$<\omega_i\omega_i>^{\#}(y^+,\mathrm{Re}_\tau) \equiv \frac{<\omega_i\omega_i>}{U_0 u_\tau^3/\nu^2}$$
$$<\omega_i\omega_i>_0^{\#}(y^+) \equiv \frac{<\omega_i\omega_i>_0}{U_0 u_\tau^3/\nu^2} \qquad (10)$$
$$<\omega_i\omega_i>_1^{+}(y^+) \equiv \frac{<\omega_i\omega_i>_1}{u_\tau^4/\nu^2}$$

Regarding the vorticity dimensions as a velocity/length we interpret the length as the viscous length ν/u_τ and the velocity as either u_τ or $(u_\tau U_0)^{1/2}$.

Using the nomenclature of Eq. 10, Eq. 9 becomes.

$$<\omega_i\omega_i>^{\#} \sim <\omega_i\omega_i>_0^{\#}(y^+) + <\omega_i\omega_i>_1^{+}(y^+)\bullet\frac{u_\tau}{U_0}(\mathrm{Re}_\tau) \quad (11)$$

Since the zero-term in Eq. 11 scales with mixed variables, and the Reynolds shear stress scales only with the friction velocity, it is reasonable to assert that they are the result of different physical processes and the zero-term is inactive. On the other hand the one-term scales on the friction velocity and contains the Reynolds stress motions. Thus, it is active in Townsend's terminology, but could also contain inactive motions .

The activities causing the two terms in Eq. 11 are not necessarily independent. In closed form problems it is typical for the first term to appear in the equations governing the second term. Another effect is that competition between two terms changes the shape the results. For instance, peaks in the curves can shift in value and location with Reynolds number. An example is the shear stress peak in Fig. 3.

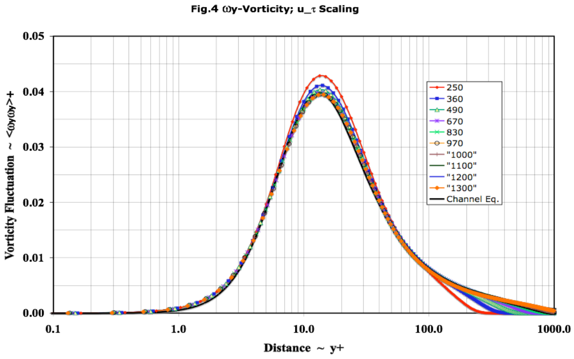

A special case, of Eq. 11 is the vertical vorticity $<\omega_y\omega_y>$ where the zero-term is absent. Figure 4 displays the profiles of $<\omega_y\omega_y>^+$ with Reynolds number as a parameter. One can see that for $Re_\tau=970$ and above, the correlation is excellent. Also plotted on this figure is the correlation obtained for channel flow in Panton (2009). The closeness of the data and the channel flow curve confirms that active motions in channels and boundary layers inner regions are the same.

However, correlations for the other two components when scaled with u_τ^4/ν^2 ($<\omega_x\omega_x>^+$ and $<\omega_z\omega_z>^+$) are not good. Figure 5 shows $<\omega_x\omega_x>^+$. At the wall there is a large value that falls off rapidly to $y^+ =1$ and then rises again to another maximum around $y^+ =20$. The solid black curve is the correlation curve for $<\omega_x\omega_x>_1^+$ determined for channel flow. The implication is that these trends arise from two physical process.

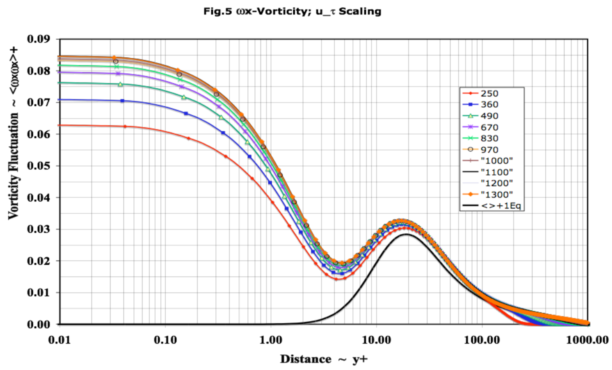

To access the proper scaling, two figures were constructed. Figure 6 displays the u_τ scaling for the values of $<\omega_x\omega_x>^+$ and $<\omega_z\omega_z>^+$ at the wall. The curves show an increase with Re_τ confirming that this is not the proper scaling. Also shown are similar data from channel flow simulations.

Fig.6 u_τ Scaling; Re Trends

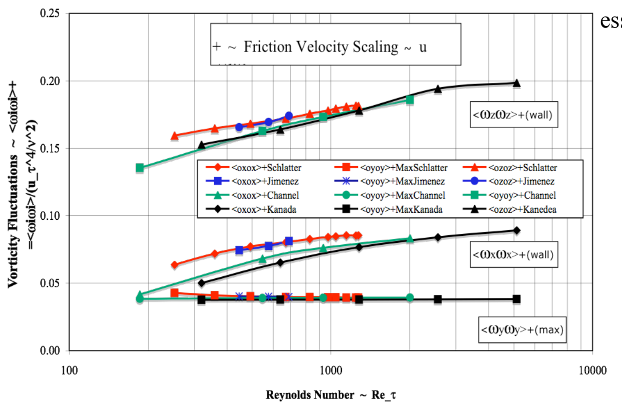

In addition, the maximum values for $<\omega_y\omega_y>^+$ are given. They are constant indicating that this is the proper scaling for $<\omega_y\omega_y>^+$.

The same vorticity is displayed in mixed scaling $(U_0\ u_\tau)^{1/2}$ on Fig. 7. The curves are reasonably constant. However, the ω_z vorticity still has a slight downward trend. It would be useful to have data at higher Reynolds numbers and from different sources .

Fig.7 U_o * u_τ Scaling; Re Trends

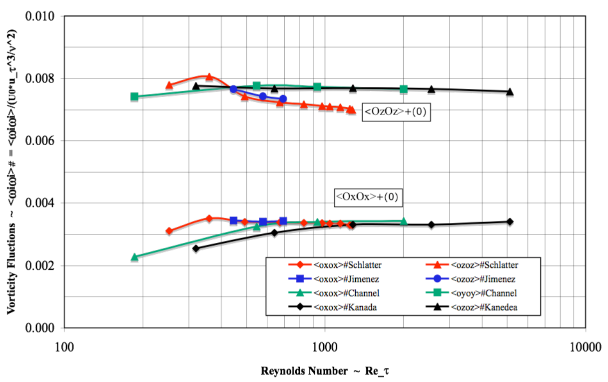

Fig.8 ωx Mixed Scaling #

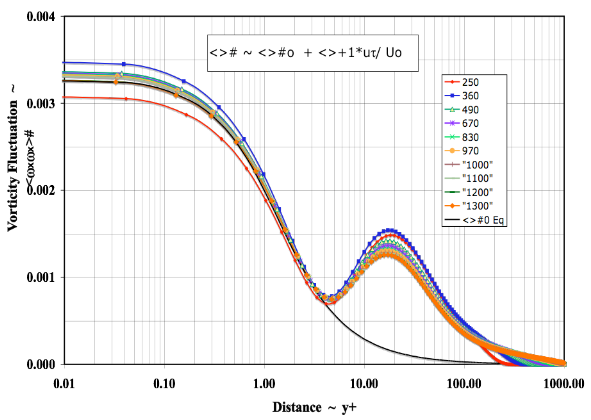

On Fig. 8 the $<\omega_x\omega_x>^\#(y^+)$ curves are shown for various Reynolds numbers. The data correlates well for low y^+, but the peak that occurs about $y^+=15$ continues to decrease with *Re*. The solid black line an estimate for the behavior as very high *Re*. This is essentially a guess for the first term in Eq. 11.

Fig.9 ωx "Active" Term

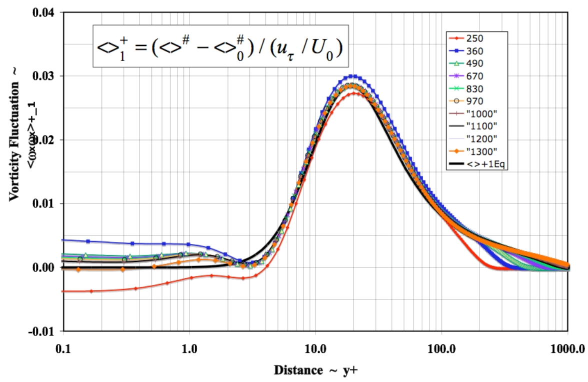

In principle, the second term in Eq. 11 is found from:

$$<\omega_i\omega_i>_1^+(y^+) \sim \left[<\omega_i\omega_i>^\# - <\omega_i\omega_i>_0^\#\right] \div \frac{u_\tau}{U_0} \quad (12)$$

The data after processing by Eq. 12 are shown on Fig. 9. The correlation is good. The solid black line is an estimate for channel flow data. It fits well except near $y^+= 4$.

Fig.10 ωz Mixed Scaling #

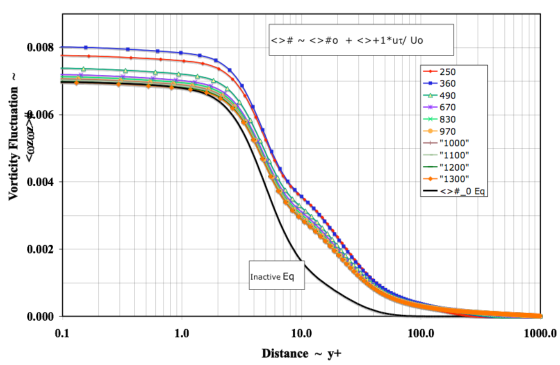

Charts similar to Figs. 8 and 9 are shown as Figs. 10 and 11 for $<\omega_z\omega_z>^\#$ and $<\omega_z\omega_z>_1^+$. The solid lines are estimates for the limiting behavior. It is essentially the second term in Eq. 11. The proper trends are again observed.

Fig.11 ωx "Active" Term

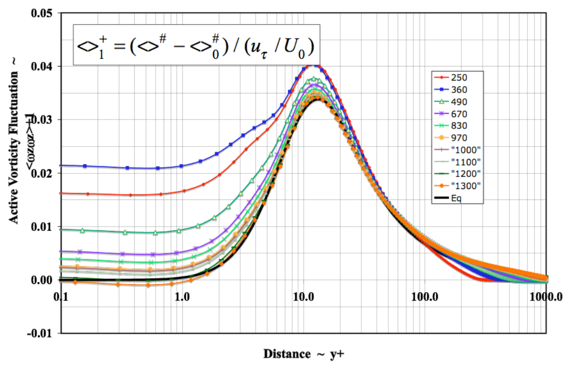

Fig 13 ωx Outer Kolmogorov Scaling; Common

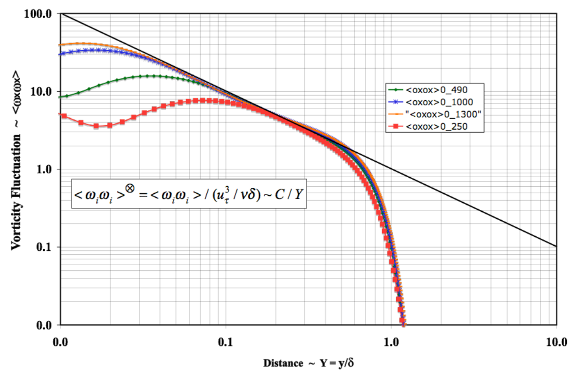

OVERLAP REGION

The zero-term in Eq. 11, which exists for the x and z-direction vorticity components, decays to zero exponentially. Therefore there is no matching term in the outer region. The vorticity generated at the wall by the potential components scrubbing the wall does not diffuse into the outer region.

Fig.12 ωx Inner Overlap Common Part

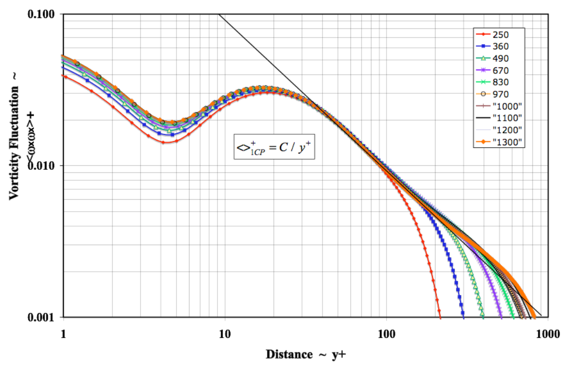

A log-log plot of $<\omega_x\omega_x>^+$ is given as Fig. 12. Curves for various Reynolds numbers collapse in an overlap region that has a minus-one slope. This is typical of all vorticity components. The common parts are:

$$<\omega_i\omega_i>_{CP}^+ = C/y^+ \qquad (13)$$

If the common part has a minus-one slope there must be a change in scale between the inner and outer regions. The proper scaling in the outer region is

$$<\omega_i\omega_i>^{\otimes} = <\omega_i\omega_i>/(u_\tau^3/\nu\delta) \qquad (14)$$

In outer variables Eq. 13 is

$$<\omega_i\omega_i>_{CP}^{\otimes} = C/Y \qquad (15)$$

Figure 13 is a log-log plot of $<\omega_x\omega_x>^{\otimes}$ in the outer variable Y. The minus-one common part is evident.

OUTER REGION

The convergence of curves for various Reynolds number is shown in Fig. 14 for $<\omega_x\omega_x>^{\otimes}$. Other components converge similarly and are not shown. Recall that the Kolmogorov time scale is $\tau = \sqrt{\nu\delta/u_\tau^3}$. Thus, the outer vorticity is scaled by $1/\tau^2$, implying that dissipation is the dominant process.

All three vorticity components are given in the outer variables on Fig. 15. The curves are for Re_τ=1300 and therefore represent the limiting values for high Reynolds numbers. It is observed that the $<\omega_y\omega_y>$ curves are about 15 % higher than the other components that are nearly the same.

Fig 14 ωx Outer Kolmogorov

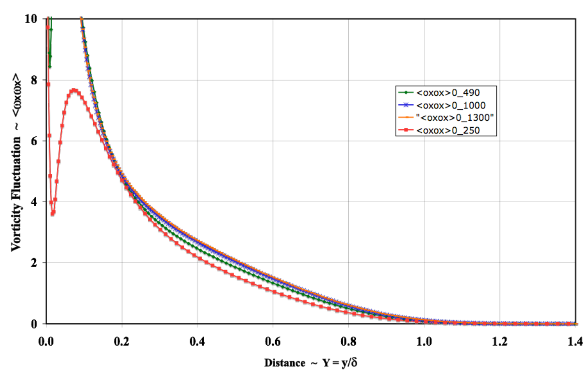

Fig. 15 ωx ωy ωz Outer Kolmogrov Scaling

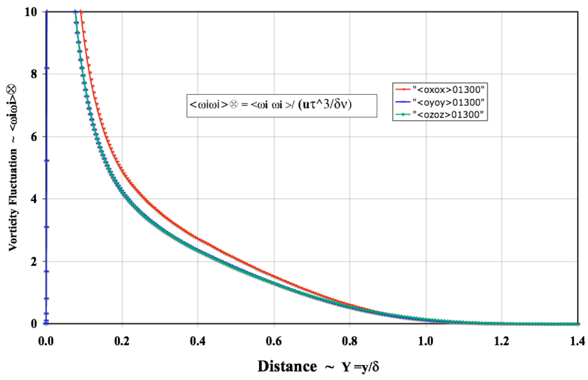

Fig.17 Second term +

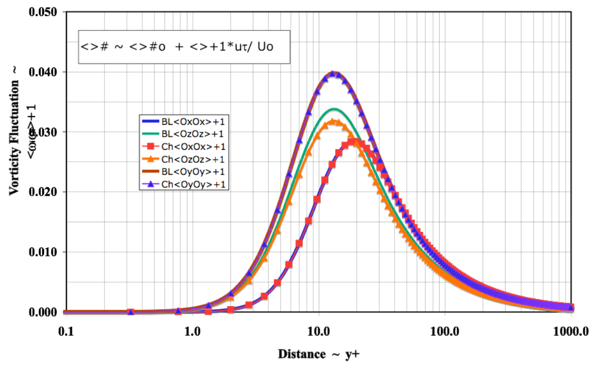

SUMMARY

An asymptotic expansion of vorticity fluctuations in the inner region requires two terms as given in Eq. 11.

$$<\omega_i\omega_i>^{\#} \sim <\omega_i\omega_i>^{\#}_0 (y^+) + <\omega_i\omega_i>^{+}_1 (y^+) \bullet \frac{u_\tau}{U_0}(\mathrm{Re}_\tau) \quad (11)$$

The first is scaled with the mixed velocity $\sqrt{U_0 u_\tau}$ while the second scales with u_τ. An exception is the vertical vorticity which has only the second term. It is proposed that the $\sqrt{U_0 u_\tau}$ scaling is the viscous response to potential fluctutions scrubing the wall. This decays exponentially in y^+ and extends to about $y^+ = 50$. Estimates for the first terms are shown in Fig.16 for boundary layers and channels. Since potential flows are often associated with the outer layer the similarity is not expected

Fig.16 First term <>#0

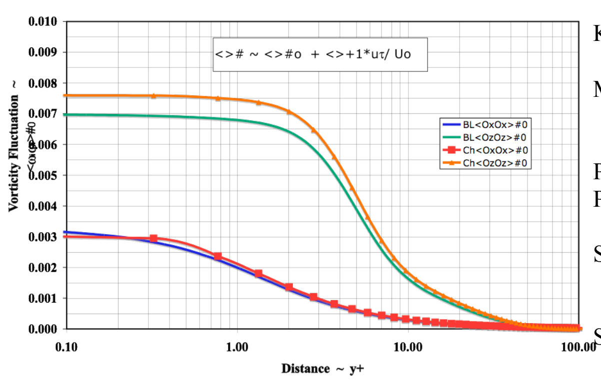

The second term scales with the friction velocity and contains the Reynolds shear stress active motions. Estimated behaviors are displayed in Fig. 17. The difference between boundary layers and channel flows are inconsequential and the channel flow estimates adequately describe the boundary layer behavior. Although the $<\omega_y\omega_y>^+$ curves must be zero at the wall, it is an assumption with respect to the other components. As the curves approach the overlap region they all obey the overlap law C/y^+

The proper scaling in the outer region is $<\omega_i\omega_i>^{\otimes} = <\omega_i\omega_i> / (u_\tau^3 / \nu\delta)$. This scaling is the Kolmogorov time scale. In order to change scaling between the regions, the overlap law for all components is C/y^+ in inner variables and C/Y in outer variables.

REFERENCES

Alfredsson, P. H. and A. V. Johansson (1984), *Phy. Fluids* **27,** p.1974.
DeGraaff, D. B. and J. K. Eaton (2000) *J. Fluid Mech.* **422**, p. 319.
Del Álamo, J. C. and J. Jiménez (2003), *Phy. Fluids,* **15,** pp L41-L44.
Del Álamo, J. C., Jiménez, J. Zandonade, P. and R. D. Moser, (2004) *J. Fluid Mech.* **500**, p.135.
Hoyas, S. and J. Jiménez (2006) *Phys. Fluids,* **18**, 011702.
Jiménez, J. and S. Hoyas (2008)," *J. Fluid Mech.* **611**, p 215.
Jiménez, J., Hoyas, S., Simens, M. P., and Y. Mizuno , (2010) *J. Fluid Mech.* **657,** p 335.
Kim, J., Moin, P. and R. D. Moser (1987), *J. Fluid Mech.* **177,** p. 133.
Morishita, K., Ishihara, T. and Y. Kaneda, (2011), Journal of Physics: Conference series.Vol 318, 022016.
Panton, R. L.(2009) *Phys. Fluids,* **21**.
Pope, S. B. (2000) *Turbulent Flows* Cambridge University Press, Cambridge, UK
Schlatter, P, Orlu, R., Li, Q., Brethouwer, G., Johansson, A.V. , Alfredsson, P. H., and D. S. Henningson (2011) , TSFP-7.
Schlatter, P. and R. Orlu, (2010) J. Fluid Mech. **659**, p. 116.
Schlatter, P., R. Orlu, Q. Li, G. Brethouwer, J.H. M. Fransson, A. V. Johansson, P. H. Alfredsson, and D. S. Henningson, (2009) Phys. Fluids **21** (051702).
Spalart, P.R. (1988), *J. Fluid Mech.* **187,** pp 61–98.